Evolution of escape processes with a time-varying load

Mee H. Choi and Ronald F. Fox
School of Physics, Georgia Institute of Technology, Atlanta, Georgia 30332
(Received 29 March 2002; published 11 September 2002)

We study an escape process of a noisy particle with a time varying load. We present an effective nonperturbative method which works even when the time varying load amplitude is comparable to other parameters. It is based on the idea that for every instant of time, we know the *quasiadiabatic* eigenspectrum and the quasiadiabatic eigenfunctions of the instantaneous system. We show that when two time-varying quasiadiabatic eigenvalues in the spectrum get close to each other, the amplitudes of the quasiadiabatic eigenfuntions show an abrupt change; therefore, the escape rate is highly affected.

DOI: 10.1103/PhysRevE.66.031103 PACS number(s): 05.40.−a, 05.10.Gg, 03.65.Ge, 31.15.−p

I. INTRODUCTION

Escape phenomena from a given prescribed potential or between stable states induced by intrinsic or external fluctuations have been well studied using stochastic processes. Kramers' original work shows a characteristic time scale of transition between two stable states [1–3]. It is the strength of fluctuation and the shape of the potential which determine the escape rate.

If the escape process involves a time-dependent potential, the escape rate will be affected by the time-dependent potential along with the fluctuation strength. In this paper we consider a random walker in a time-dependent potential on a one-dimensional line (a,L). The Langevin equation in the overdamped case is

$$\dot{x} = -\frac{\partial U(x,t)}{\partial x} + \gamma(t), \tag{1}$$

where $F(t) = -\partial U(x,t)/\partial x$ is a time varying force, and γ is a Gaussian white fluctuation force. γ has a zero mean and correlation strength D,

$$\langle \gamma(t) \rangle = 0,$$

$$\langle \gamma(t)\gamma(t') \rangle = 2D\delta(t-t'). \tag{2}$$

The Fokker-Planck (FP) equation for the probability density of the particle, which is a description equivalent to the Langevin equation, can be written

$$\frac{\partial p(x,t)}{\partial t} = -\frac{\partial [F(x,t)p(x,t)]}{\partial x} + D\frac{\partial^2 p(x,t)}{\partial x^2}. \tag{3}$$

We also define $\mathcal{L}_F$ as the forward Fokker-Planck operator such that

$$\mathcal{L}_F = D\frac{\partial}{\partial x^2} - \frac{\partial [F(x,t)]}{\partial x},$$

$$\frac{\partial p(x,t)}{\partial t} = \mathcal{L}_F p(x,t). \tag{4}$$

Our specific problem here is a random walker carrying a time-dependent load. We are interested in the escape time for the walker to reach the point $x=L$ when it starts its motion at $x=a$. Therefore, we have one reflecting boundary condition at $x=a$, and one absorbing boundary condition at $x=L$. The load acts as a retarding force against the motion toward the absorbing boundary.

In the case where the load is constant in time, i.e., $F(t) = F_0$, this model has been used recently to understand the motion of the kinesin molecule moving on a microtubule [4]. Kinesin acts as a kind of biological motor, and this model can explain the speed of the motor motion as a function of load. The escape time distribution for the motor to move a discrete step was expressed as a superposition of eigenfunctions and eigenvalues of the backward Fokker-Planck operator. The escape time distribution combined with various chemical reaction rates gives an overall velocity of the motor. We found out that the time scale of the diffusive term from the load is well separated from the time scale from the fluctuations.

If the load depends on time, it necessarily introduces another time scale, such as the period of sinusoidal driving, decaying rate of load, etc. These rates affect the escape rates. The analytic solution for the time-dependent escape process is hard to obtain, and the perturbative method would be available only when the amplitude of time varying parameters are small enough compared to other exisiting ones. In this paper we present a nonperturbative method when the instantaneous eigenvalues (*quasiadiabatic eigenvalues*) of the Fokker-Planck operator at every instant of time are known. This method was originally conceived to solve time-dependent problems in quantum systems, where the time varying quasiadiabatic eigenvalue spectrum of the Hamiltonian shows nontrivial behavior [5]. For a frozen value of the external potential, the Hamiltonian has an adiabatic spectrum parametrized by the frozen external potential. When two levels in the eigenvalue spectrum approach each other closely (however, they never cross each other; avoided level crossings), the system behaves extremely nonadiabatically with level mixings.

Even though this method was used to describe the effect of slowly varying parameters in the quantum systems, the solution turned out to be applicable to a wide range of time scales. We choose a time scale for a time varying parameter

in such a way that the unperturbed escape rate and the time scale for a time varying parameter are in the same order of time scales. By doing so, the interplay of these effects will be pronounced.

For escape processes, it is more convenient to use the backward FP equation

$$\frac{\partial p(x,t)}{\partial t} = F(x,t)\frac{\partial}{\partial x}p(x,t) + D\frac{\partial^2 p(x,t)}{\partial x^2}, \tag{5}$$

and the backward FP operator, defined as

$$\mathcal{L}_B = D\frac{\partial^2}{\partial x^2} + F(x,t)\frac{\partial}{\partial x},$$

$$\frac{\partial p(x,t)}{\partial t} = \mathcal{L}_B p(x,t). \tag{6}$$

In Sec. II we present two methods using different representations, both giving the same solution for the FP equation. In one picture, we expand the general solution in the fixed eigenfunctions, and in the other, the general solution is expanded in the instantaneous eigenfunctions in time (*quasiadiabatic method*).

In Sec. III we show a specific example of a load, which varies sinusoidally in time in both pictures. We show the time-varying quasieigenvalue spectrum. When the two quasiadiabatic-eigenvalue levels approach each other, it will affect the evolution equation, and thus the escape rate.

In Sec. IV, we briefly show how the same problem can be treated by a perturbative method, and compare the results with the previous methods.

In Sec. V, by comparing the previous results with numerical simulation, we demonstrate that when the load amplitude becomes comparable to other existing parameters, the two nonperturbative pictures show a far better result than the perturbative one.

II. DIRECT TIME-DEPENDENT PICTURE VERSUS QUASIADIABATIC PICTURE

If the time-dependent load can be written as

$$F(x,t) = F_0 + F_1(x,t), \tag{7}$$

the backward FP operator also can be split into a stationary part and a time-dependent part, such that

$$\mathcal{L}_B^{stationary} = D\frac{\partial^2}{\partial x^2} + F_0\frac{\partial}{\partial x},$$

$$\mathcal{L}_B^{time\ dependent} = F_1(x,t)\frac{\partial}{\partial x}. \tag{8}$$

If we can obtain a set of eigenvalues λ, and eigenfunctions ϕ to the stationary part of the backward FP operator, i.e.,

$$\mathcal{L}_B^{stationary}\phi = -\lambda\phi, \tag{9}$$

a general solution can be written as

$$p(x,t) = \sum_{n=0}^{\infty} \alpha_n(t)\phi_n(x), \tag{10}$$

where $\alpha_n(t)$ are the time-dependent coefficients. The orthonormality condition for the eigenfunctions $\phi(x)$'s of this operator is

$$\langle \phi_n(x), \phi_m(x)\rangle = \int_a^b \phi_n(x)\phi_m(x)\omega(x)dx = \delta_{nm}, \tag{11}$$

where $\omega(x)$ is the weight function according to the Sturm-Liouville theory. During the evolution, we will expand the solution in the same basis set. If we combine Eq. (10) with Eq. (8), and Eq. (9), we get

$$\frac{d}{dt}\left(\sum_{n=0}^{\infty}\alpha_n(t)\phi_n(x)\right) = -\sum_{n=0}^{\infty}\lambda_n\alpha_n(t)\phi_n(x) + F_1(x,t)\partial_x\sum_{n=0}^{\infty}\alpha_n(t)\phi_n(x). \tag{12}$$

Using the orthonormality from Eq. (11) and the fact that $\phi_n(x)$ are not time dependent, we finally obtain a set of ordinary differential equations for $\alpha_m(t)$, i.e.,

$$\dot{\alpha}_m(t) = -\lambda_m\alpha_m(t) + \sum_n \langle \phi_m, F_1(x,t)\partial_x\phi_n\rangle\alpha_n(t). \tag{13}$$

There is no restriction for $|F_1(x,t)|$ in terms of other parameters here. We call this method *the direct time-dependent method*, and we only have to know the eigenspectrum for the $F_1(x,t)=0$ case.

As an alternative perspective, for a given instant of time $t=t'$, the force $F(t)$ is given by f'. Let us assume that with this frozen value, we can obtain a set of eigenvalues of $\tilde{\lambda}_n$ for the operator

$$\tilde{\mathcal{L}} = f'\frac{\partial}{\partial x} + D\frac{\partial}{\partial x^2}, \tag{14}$$

and we have

$$\frac{\partial p(x,t)}{\partial t} = -\tilde{\lambda}p(x,t). \tag{15}$$

A general solution will be written as

$$p(x,t) = \sum_{n=0}^{\infty}\tilde{\alpha}_n(t)\tilde{\phi}_n(x,t), \tag{16}$$

where $\tilde{\alpha}_n(t)$ are the time-dependent coefficients. Note that $\tilde{\phi}_n(x,t) = \tilde{\phi}_n(x,f';t)$ are also time varying in time. In this picture we expand a general solution in time varying quasiadiabatic eigenfunctions, and the dynamics can be observed

from the eigenfunctions at that instant. This picture can have an advantage when we want to view the dynamics from the moving eigenstates. If we take the derivative of Eq. (16), we get

$$\partial_t \sum_{n=0} \tilde{\alpha}_n(t)\tilde{\phi}_n(x,t) = \sum_{n=0} \dot{\tilde{\alpha}}_n(t)\tilde{\phi}_n(x,t) + \sum_n \tilde{\alpha}_n(t)\partial_{f'}\tilde{\phi}_n(x,f';x)\frac{df'}{dt}. \tag{17}$$

We call this method the quasiadiabatic method. The relations for the amplitudes from the two different pictures are given as

$$\tilde{\alpha}_m(t) = \left\langle \tilde{\phi}_m(x,t) \middle| \sum_n \alpha_n \phi_n(x) \right\rangle,$$

$$\alpha_m(t) = \left\langle \phi_m(x) \middle| \sum_n \tilde{\alpha}_n(t)\tilde{\phi}_n(x,t) \right\rangle. \tag{18}$$

Since the random walker starts out at $x=a$, normally the initial distribution function is sharply peaked around $x=a$, such as a delta function. We therefore set (in the direct time-dependent method),

$$p(x,t) = \sum_{n=0} \exp(-\lambda_n t)\phi_n(x)\phi_n(x_0). \tag{19}$$

(A finite number of eigenfunctions with the corresponding expansion coefficients give only an approximation.) For $t=0$, the above distribution reduces to

$$p(x,t=0) = \sum_n^{\infty} \phi_n(x)\phi_n(x_0) = \delta(x-x_0). \tag{20}$$

The probability that the particle stays in $[a,b]$ when the initial distribution is $\delta(x-x_0)$; $G(x_0,t)$ is to be calculated as

$$G(x_0,t) = \int_0^{\infty} \phi_n(x_0)dx_0 \exp(-\lambda_n t)\phi_n(x). \tag{21}$$

The escape rate distribution is defined as

$$Pv(t) = -\partial_t G(x_0,t). \tag{22}$$

III. PERIODIC DRIVING

The effect of a time-dependent periodic forcing on a diffusion process with a force-free potential in two absorbing boundary conditions was analyzed in the 1980 [8]. In Ref. [8], a simple random walker (without any particular potential) under a periodic forcing diffuses along a one-dimensional (1D) line segment. It is shown that there is a resonance frequency which minimizes the mean first passage time (MFPT), and at this resonance frequency, it has a linear dependence on the lattice size L.

In this section the random walker walks along a 1D segment with a load (retarding force) and periodic forcing. We have one absorbing and one reflecting boundary condition. Without a time-dependent oscillating part, the load in our case would always act against the forward motion. With the oscillating part of the load, the load helps the motion half of the period and deters the motion the other half of the period. A similar model was used to examine the effect of the time varying current on the histogram of spikings in the excitable systems [6].

We first consider a constant load $-F_0$. The backward FP operator is written

$$\mathcal{L}_B\phi = -\lambda\phi,$$

$$\mathcal{L}_B = D\frac{\partial^2}{\partial x^2} - F_0\frac{\partial}{\partial x}. \tag{23}$$

The corresponding boundary conditions are

$$p(x,t)|_{x=L} = 0 \tag{24}$$

for the absorbing boundary condition, and

$$\partial_x p(x,t)|_{x=a} = 0 \tag{25}$$

for the reflecting boundary condition. The solution $p(x,t)$ will be of a form with $\exp(-\lambda_n t)\phi_n(x)$. With the two boundary conditions for $x=a$, $x=L$, eigenfunctions $\phi_n(x)$ are obtained such that

$$\phi_n(x) = \exp\left(-\frac{F_0 x}{2D}\right) b_n(x), \tag{26}$$

with

$$b_n(x) = \sin[k_n(x-L)] \quad \text{for } \frac{2D}{F_0 L} > 1, \tag{27}$$

and

$$b_1(x) = \begin{cases} \sinh[k_n(x-L)] & \text{for } \dfrac{2D}{F_0 L} < 1, \\ 1 - \dfrac{x}{L} & \text{for } \dfrac{2D}{F_0 L} = 1. \end{cases} \tag{28}$$

A set of k_n is to be obtained from a transcendental equation

$$\tan(k_n L) = \frac{2D}{F_0 L} k_n L \quad \text{for } \frac{2D}{F_0 L} > 1 \tag{29}$$

and $\tanh(k_1 L) = (2D/F_0 L)k_1 L$ for $(2D/F_0 L) < 1$, $k_1 = 0$ for $2D/F_0 L = 1$. Eigenvalues λ_n satisfy the relation depending on the conditions

$$\lambda_n = \frac{F_0^2}{4D} + Dk_n^2 \quad \text{for } \frac{2D}{F_0 L} > 1, \tag{30}$$

and

$$\lambda_1(x)=\begin{cases}\dfrac{F_0^2}{4D}-Dk_n^2 & \text{for } \dfrac{2D}{F_0L}<1,\\ \dfrac{F_0^2}{4D} & \text{for } \dfrac{2D}{F_0L}=1.\end{cases} \tag{31}$$

The orthonormality condition for this specific problem is

$$\langle \phi_n(x),\phi_m(x)\rangle=\int_a^L \phi_n(x)\phi_m(x)\exp\left(-\frac{F_0}{D}x\right)dx=\delta_{nm}. \tag{32}$$

Here, we have the weight function

$$\omega_n(x)=\exp\left(-\frac{F_0}{D}x\right)dx. \tag{33}$$

If we apply a periodic perturbation, the backward FP equation has an additional term such that

$$\frac{\partial p}{\partial t}=[-F_0-\epsilon\sin(\omega t+\phi_0)]\partial_x p+D\frac{\partial p}{\partial x^2}, \tag{34}$$

where ω is the driving frequency and $\epsilon \ll F_0$ in our case. This equation implies that we have careful control of the driving phase, and when escape takes place, the next random walker starts with the same initial condition as the previous one. In other words, we reset to a known phase for each escape process. In practice, an observer does not have control of the phase. Another diffusion process starts being recorded where the earlier random walker left off in the phase. It is best to phase average the solution to obtain meaningful statistics. For instance, a driven escape process out of a double well with proper phase averaging was studied in [7]. To simplify matters, we reset the initial phase for every ensemble sample, i.e., $\phi_0=0$.

With this additional time-dependent part $-\epsilon\sin(\omega t+\phi_o)$, differential equations for α_m for the direct time-dependent method are given as

$$\dot{\alpha}_m(t)=-\lambda_m\alpha_m(t)-\epsilon\sin(\omega t)\times\sum_n\int_a^b \phi_m'(x)\exp\left(-\frac{F_0x}{D}\right)\partial_x\phi_n(x)dx \tag{35}$$

and

$$\dot{\tilde{\alpha}}_m(t)=-\tilde{\lambda}_m\tilde{\alpha}_m(t)-\sum_n\int_a^b \tilde{\phi}_m'(x,f';t)\times\exp\left(-\frac{f'x}{D}\right)\partial_{f'}\tilde{\phi}_n'(x,f';t)dx\frac{df'}{dt}, \tag{36}$$

for the quasiadiabatic method, where

$$f'=-F_0-\epsilon\sin(\omega t+\phi_0), \tag{37}$$

$$\frac{df'}{dt}=-\omega\epsilon\cos\omega t. \tag{38}$$

As in quantum systems [9], we can also calculate the quasieigenvalue spectrum as we move along time. A full set of eigenvalue levels are calculated from Eqs. (29), (30). With two levels only, say the two lowest levels, we can set up a matrix for $f'=\Delta=-\epsilon\sin(\omega t)$ in the basis of $f'=0$

$$\begin{bmatrix}\lambda_1-\Delta\langle\xi_1|\partial_x\xi_1\rangle & -\Delta\langle\xi_1|\partial_x\xi_2\rangle\\ -\Delta\langle\xi_2|\partial_x\xi_1\rangle & \lambda_2-\Delta\langle\xi_2|\partial_x\xi_2\rangle\end{bmatrix}. \tag{39}$$

If we diagonalize this matrix, we obtain a quadratic equation which will give us two quasiadiabatic eigenvalues, i.e.,

$$\lambda^2-(\lambda_1+\lambda_2-\Delta\langle\xi_1|\partial_x\xi_1\rangle-\Delta\langle\xi_2|\partial_x\xi_2\rangle)\lambda+(-\lambda_1+\Delta\langle\xi_1|\partial_x\xi_1\rangle)(-\lambda_2+\Delta\langle\xi_2|\partial_x\xi_2\rangle)+\Delta^2\langle\xi_1|\partial_x\xi_2\rangle\langle\xi_2|\partial_x\xi_1\rangle=0. \tag{40}$$

IV. ADIABATIC METHOD

A perturbative method assumes a solution

$$p=p_0+\epsilon p_1+\epsilon^2 p_2+\cdots. \tag{41}$$

This assumption turns Eq. (3) into a set of equations

$$\begin{aligned}Dp_{0_{xx}}-F_0p_{0_x}-p_{0_t}&=0,\\ Dp_{1_{xx}}-F_0p_{1_x}-p_{1_t}&=\sin(\omega t)p_{0_x},\\ Dp_{2_{xx}}-F_0p_{2_x}-p_{2_t}&=\sin(\omega t)p_{1_x}\cdots,\end{aligned} \tag{42}$$

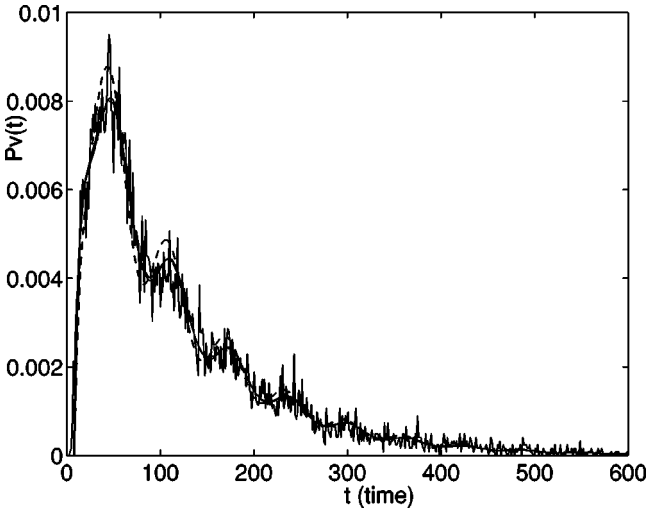

FIG. 1. The escape time distribution with a sinusodial load is plotted up to ten driving periods. $D=0.6$, $F_0=0.1$, $a=0$, $L=9$, $\epsilon=0.03$, $\omega=0.1$. The noisy line is the numerical simulation of 10^4 ensembles and the solid lines are from three analytical results. The dashed curve (higher one) is from the perturbative method; the solid ones (lower curves) (they overlap each other) are results from the nonperturbative methods. We used up to λ_2,ϕ_2 for nonperturbative methods, which was sufficient since the λ_n are separated enough, and we calculated the first order correction $O(\epsilon)$ for the perturbative method. The next higher one does not show much improvement.

where subscripts denote partial derivatives. Each equation is in ϵ^0, ϵ^1, ϵ^2 order, respectively. We assume a general solution

$$p_i = \sum_n \alpha_n^{(i)}(t)\phi_n(x). \tag{43}$$

The right-hand side of Eq. (42) can be rewritten as

$$\sin(\omega t)p_{0_x} = \sum_n C_n \exp(-\lambda_n t)\sin(\omega t)\partial_x \phi_n(x)$$

$$= \sum \beta_n(t)\phi_n(x), \tag{44}$$

where

$$\beta_n(t) = \sum C_m \exp(-\lambda_m t)\sin(\omega t)\langle \phi_n(x), \partial_x \phi_m(x)\rangle. \tag{45}$$

For first order, we obtain for $\alpha^{(1)}(t)$

$$\alpha_n^{(1)}(t) = -\exp(-\lambda_n t)\int_0^t \exp(-\lambda_n t) \times \sum_m C_m \exp(-\lambda_m t)\sin(\omega t) \times \langle \phi_n(x), \partial_x \phi_m(x)\rangle dt. \tag{46}$$

With this obtained result of p_1, we can substitute the solution p_1 in Eq. (42) and repeat the same procedure for equations of higher orders until the solution converges. When the amplitude is small enough, the result works well, even in first order.

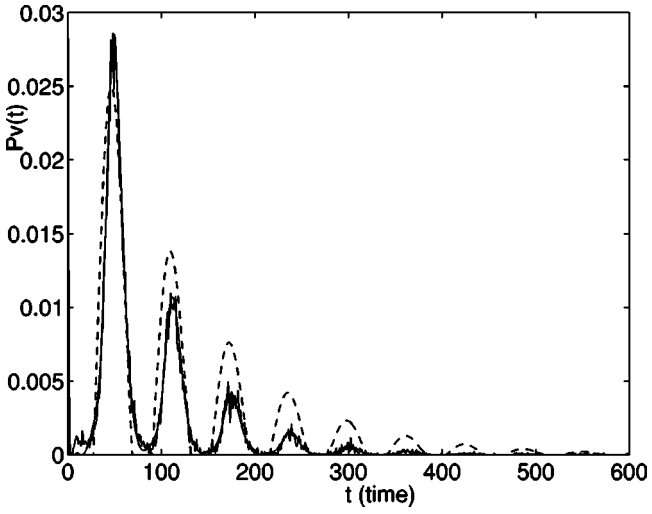

FIG. 2. The escape time distribution with a sinusodial load is plotted for up to ten driving periods. $D=0.6$, $F_0=0.1$, $a=0$, $L=9$, $\epsilon=0.3$, $\omega=0.1$. The noisy line is the numerical simulation of 10^4 ensembles and the solid lines are from nonperturbative methods. The dotted line is from the perturbative method. Here note that $\epsilon > F_0$. We used five eigenvalues and eigenfunctions for the expansion for the direct time-dependent and quasiadiabatic method, and used the first order correction for the perturbative method.

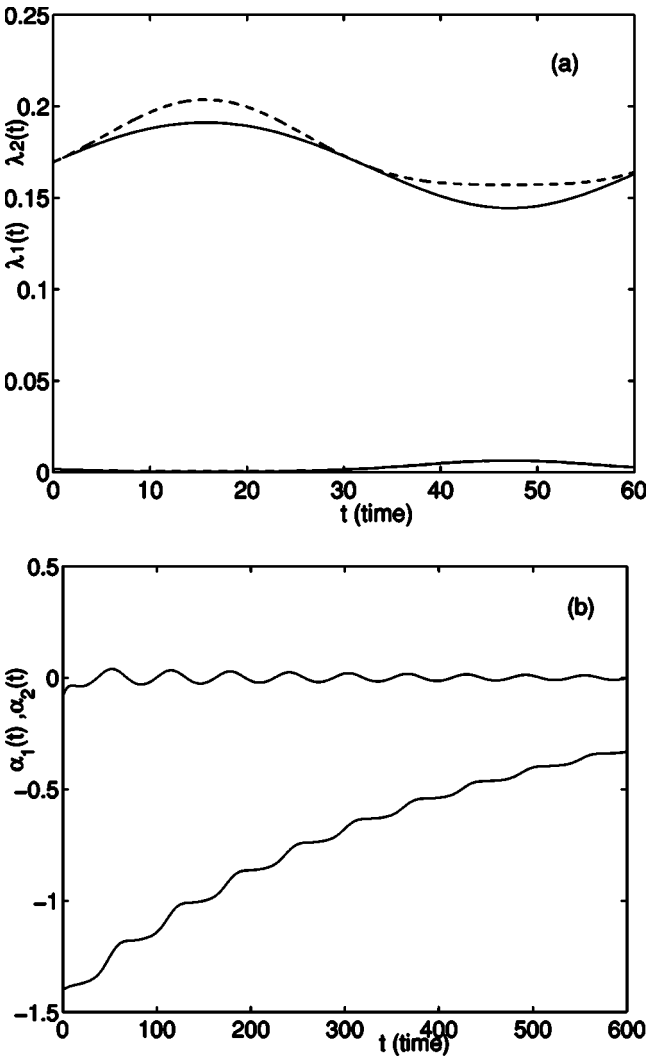

FIG. 3. (a) The first two quasiadiabatic eigenvalue curves in time (for one period). The parameters are $D=0.6$, $F_0=0.3$, $a=0$, $L=9$, $\epsilon=0.15$, $\omega=0.1$. The dotted lines are from the 2×2 matrix approximation from Eq. (40), and the solid line is from directly solving Eq. (30). The levels get close to each other when the periodic driving becomes less retarding. (b) The amplitudes for the first two levels from the direct time-dependent method are shown. $\alpha_1(t)$ (lower one) shows an abrupt change in value (a steplike shape) in every period when the quasiadiabatic levels approach each other the closest. This change is reflected in the escape time distribution.

V. NUMERICAL RESULTS

In numerical simulations, we used a Box-Müller algorithm for a Gaussian stochastic force and used a Monte Carlo method with 10^4 ensembles. In Fig. 1 we show the escape time distribution for $D=0.6, F_0=0.1, a=0, L=9, \epsilon=0.03, \omega=0.1$. The numerical simulation was compared with the direct time-dependent method, the quasiadiabatic method, and the perturbative method, respectively. The λ_n are well sepa-

rated in terms of the time scale, and we used only the first two eigenvalues and eigenfunctions for the backward FP operator. In this case, $|F_0| \geqslant \epsilon$, and all three methods compare relatively well with the simulation. In Fig. 2 we show the escape time distribution for $D=0.6, F_0=0.1, a=0, L=9, \epsilon=0.09, \omega=0.1$. ϵ is comparable in magnitude to F_0 and the nonperturbative methods show a far better result compared to the perturbative method. In Fig. 3(a) we show the first two adiabatic eigenvalue levels in time for a period which was calculated directly from Eq. (30) and the two level approximation from Eq. (40) for $D=0.6, F_0=0.1, a=0, L=13, \epsilon=0.2, \omega=0.1$. When the two levels approach each other, we see the increased escape rate (a peak in the escape rate) around the time. This is also when the load becomes least retarding. The quasispectrum gives us an idea of how the escape rate changes according as the time-dependent forcing changes. In Fig. 3(b) we plot the first two amplitudes, i.e., $\alpha_1(t), \alpha_2(t)$ in the direct time-dependent picture. Their rate of change affects directly the rate of escape process. We see an abrupt change in value at every period of the forcing (a steplike behavior) in $\alpha_1(t)$, when the quasiadiabatic levels approach each other.

VI. CONCLUSION

We considered a noisy particle moving under carrying a time varying load on a 1D segment. The time varying load in this case is periodic in time. We used one absorbing condition and one reflecting condition and measured the escape time when the particle approaches the absorbing boundary condition once it start at the reflecting position. The load acts against the motion of the random walker. The escape time distribution was solved using the backward Fokker-Planck equation and was compared with numerical simulations.

We discussed two nonperturbative methods for solving the FP equation. In one case, the solution is expanded in the fixed eigenfunctions of the FP operator, and in the other, the eigenfuctions change in time. The quasiadiabatic eigenvalue spectrum levels show the dynamics of the system. When the two levels closely approach each other, the escape rate is more pronounced. This behavior is very similar to the quantum systems where the two adiabatic eigenvalue levels show abrupt level mixings.

We derived a set of ordinary differential equations for the time-dependent amplitudes for the fixed or moving eigenfunctions. Both methods using fixed and moving eigenfunctions are compared with the numerical simulations. We show the validity of these methods when the time-dependent parameter is comparable in magnitude to other parameters for the system. We find these methods far better than the perturbative one. If the particle is in a nonlinear potential, these methods will provide good insight for the escape rate.

Prediction of rate processes is traditionally given by the inverse of the first eigenvalue of the Fokker-Plank operator. When the time-dependent driving term is introduced, it is desirable to find how this eigenvalue will be modified by this perturbation. This analytical approach also gives an insight into the evolution of time-dependent amplitudes which are closely related to the escape rates. They cannot be separately obtained from the numerics.

We find this method quite effective since it converts the partial differential equation to a set of ordinary equations. When the time scale becomes long or the amplitude becomes large, the numerical method should consider an adjustable grid size. In this method this consideration is not necessary.

ACKNOWLEDGMENTS

M.H.C thanks Markus De Shon for reviewing the manuscript along with valuable comments. The work was supported by National Science Foundation Grant No. PHYS-9819646.

[1] C.W. Gardiner, *Handbook of Stochastic Methods* (Springer-Verlag, Berlin, 1989).
[2] H. Risken, *The Fokker-Planck Equation* (Springer-Verlag, Berlin, 1989).
[3] H.C. Tuckwell, *Introduction to Theoretical Neurobiology* (Cambridge University Press, Cambridge, 1988), Vol. 2.
[4] R.F. Fox and M.H. Choi, Phys. Rev. E **63**, 051901 (2001).
[5] R.F. Fox and P. Jung, Phys. Rev. A **57**, 2339 (1998).
[6] A.R. Bulsara, T.C. Elston, C.R. Doering, S.B. Lowen, and K. Lindenberg, Phys. Rev. E **53**, 3958 (1996).
[7] M.H. Choi, R.F. Fox, and P. Jung, Phys. Rev. E **57**, 6335 (1998).
[8] J.E. Fletcher, S. Havlin, and G.H. Weiss, J. Stat. Phys. **51**, 215 (1988).
[9] F. Haake, *Quantum Signatures of Chaos* (Springer-Verlag, Berlin, 1991).